Diagonal charge-density-wave state in the insulating spin-glass phase of $La_{2-x}Sr_xCuO_4$

O. P. Sushkov
School of Physics, University of New South Wales, Sydney 2052, Australia
(Received 30 March 2008; published 6 May 2008)

We show that due to the Dzyaloshinskii-Moriya and the *XY* anisotropies, the disordered diagonal spin spiral in the insulating $La_{2-x}Sr_xCuO_4$ generates a diagonal charge density wave (CDW) with the wave vector twice that of the spin spiral. The amplitude of the CDW depends on values of the anisotropies, the doping level, and the density of states at the chemical potential. Based on available experimental data, we estimate that for 4% doping, the amplitude of CDW is about 1/10 of the doping level. We believe that this mechanism explains the CDW recently observed in Zn-codoped detwinned $La_{2-x}Sr_xCuO_4$.

DOI: 10.1103/PhysRevB.77.193103 PACS number(s): 74.72.Dn, 71.45.Lr, 75.30.Fv, 75.50.Ee

The problem of charge density waves or charge stripes is one of central importance in the physics of cuprates. The effect was first discovered more than a decade ago[1] (see also Ref. 2) and has been intensively studied since then. The effect has only been observed in two cuprates, $La_{1.875}Ba_{0.125}CuO_4$ and $La_{1.6-x}Nd_{0.4}Sr_xCuO_4$, only in the low-temperature tetragonal (LTT) phase, and only at doping close to $x=0.12$. A very recent study[3] has revealed a charge density wave (CDW) in absolutely different conditions. The compound is $La_{1.95}Sr_{0.05}Cu_{0.95}Zn_{0.05}O_4$, the phase is the low-temperature orthorhombic (LTO), and the doping level is about $x=0.04-0.05$. We believe that this discovery provides a very important insight into the problem of charge stripes. In this Brief Report, we suggest a specific mechanism for CDW in the spin-glass LTO phase.

The three-dimensional antiferromagnetic Néel order in $La_{2-x}Sr_xCuO_4$ (LSCO) disappears at doping $x\approx 0.02$ and gives way to the so-called spin-glass phase, which extends up to $x\approx 0.055$. In both the Néel and the spin-glass phase, the system essentially behaves as an Anderson insulator.[4,5] Superconductivity then sets in for doping $x\gtrsim 0.055$. The incommensurate magnetic order has been observed at low temperature in neutron scattering. This order manifests itself as a scattering peak shifted with respect to the antiferromagnetic position. In the spin-glass phase, the shift is directed along the *b* axis and linearly scales with doping.[6] In the underdoped superconducting region ($0.055\lesssim x\lesssim 0.12$), the shift still scales linearly with doping, but it is directed along one of the crystal axes of the tetragonal lattice.[7]

In the present work, we address the insulating spin-glass phase. The theory for the *spin structure* of the insulating phase has been developed in Refs. 8–10. The theory is based on the idea of the disordered spin spiral. Intrinsically, this picture does not contain any charge ordering and this is qualitatively different from the stripe scenario.[11] In the present work, we demonstrate that a small charge modulation is still possible in the spin spiral picture due to the spin-orbit interaction. We show also that this effect perfectly explains the experimental data.

Outlines of the spin structure description. (1) Due to strong antiferromagnetic correlations, the minima of dispersion of a mobile hole are at points $(\pm\pi/2,\pm\pi/2)$ of the Brillouin zone, so the system can, to some extent, be considered as a two valley semiconductor. The hole does not have a usual spin, but it possesses a pseudospin that describes how the hole wave function is distributed between two magnetic sublattices. (2) At low temperature, each hole is trapped in a hydrogenlike bound state near the corresponding Sr ion, the binding energy is about 10–15 meV, and the radius of the bound state is about 10 Å. (3) Due to the orthorhombic distortion of LSCO, the *b* valley $(-\pi/2,\pi/2)$ is deeper than the *a* valley $(\pi/2,\pi/2)$. So, all the hydrogenlike bound states are built with holes from the *b* valley. In what follows, we refer to these bound states as impurities. (4) Each impurity creates a spiral distortion of the spin background in the orthorhombic *b* direction. The distortion is observed in neutron scattering. So, the state is not a simple spin glass; it is a disordered spin spiral. (5) At the point of overlapping of bound states ("percolation" point), the direction of the spiral must rotate from the diagonal to parallel because of the Pauli principle. Simultaneously, the superconducting pairing is getting possible. Hence, $x=0.055$ is the percolation point.

Spiral pitch. Calculation of the spiral pitch can be performed within the mean-field approximation. Mobile holes are trapped by Sr ions in hydrogenlike bound states ("impurities"). The ground state of the "hydrogen atom" is fourfold degenerate: (twofold pseudospin)$\times$(twofold valley). The orthorhombic distortion lifts the valley degeneracy, so all the impurities reside in the *b* valley.[9,12] Impurity pseudospin interacts with the spiral distortion of the spin fabric.[8] The interaction energy is $\sqrt{2}gQ_b$, where $\mathbf{Q}$ is the wave vector of the spiral, Q_b is the component along the orthorhombic *b* direction, and the coupling constant is approximately equal to the antiferromagnetic exchange, $g\approx J\approx 140$ meV. We set the tetragonal lattice spacing equal to unity, so the wave vector Q is dimensionless. The pseudospin degeneracy is lifted as soon as the spiral is established; all pseudospins are aligned and the corresponding energy gain per unit area is $-x\sqrt{2}gQ$. Here, x is the concentration of impurities that is practically equal to doping. The elastic energy of the spin fabric deformation is $\rho_sQ^2/2$. Here, $\rho_s\approx 0.18$ J is the spin stiffness. Thus, the total energy is $\rho_sQ^2/2-x\sqrt{2}gQ_b$. Minimization with respect to Q gives

$$Q=Q_b=\frac{\sqrt{2}g}{\rho_s}x. \tag{1}$$

To fit the experimental data,[6] we need $g=0.7$ J that agrees with the *t-J* model estimate, $g\approx J$. The presented mean-field

picture does not address the stability of the state, broadening of the line due to disorder, topological defects, etc. These issues have been studied in Refs. 9 and 10. The stability depends on the localization length (size of the impurity) that does not appear in the mean-field picture. However, as soon as we know that the disordered spiral state is stable, then the above description is correct. We would like to stress that the spiral picture does not necessary assume a static spiral. The spiral can be dynamic. In particular, in a pure two-dimensional (2D) system, the spiral is dynamic at any nonzero temperature. In LSCO, due to anisotropies and a weak three-dimensional coupling, the spiral becomes dynamic at a small finite temperature, $T \sim 20$ K. However, the absence of the static spiral at $T \geq 20$ K does not mean that the spiral is not there; it just becomes dynamic. The important components in the above picture are (1) the hole binding, (2) the a-valley depopulation, and (3) the height of the spin-wave dome E_{cross} observed in neutron scattering. Both the binding energy and the valley anisotropy energy are about 10–15 meV.[8,12] The value of E_{cross} depends on doping, and for $x=0.03-0.05$, it is also about 15 meV.[13] Therefore, the spiral description is valid up to characteristic temperature $T_h \sim 150$ K.

Density of states. In the case of uniform doping, the diagonal spiral (unlike the parallel spiral) always has a tendency toward charge modulation.[14,15] In the case of the disordered state, the problem of charge instability was resolved in Refs. 8–10 assuming that at zero temperature all the Sr-hole bound states are filled and, hence, there is no room for compression. So, implicitly, the picture of energy levels shown in Fig. 1(a) was assumed: all the bound states are below the chemical potential.

However, this picture would imply the activation behavior of dc conductivity $\sigma \propto \exp[-(\Delta E/T)]$, while it is well established that the conductivity follows the 2D version of the Mott variable range hopping (VRH) formula,[4]

$$\sigma \sim \exp[-(T_0/T)^{1/3}]. \tag{2}$$

This implies that the chemical potential is within the range of impurity energies, as shown in Fig. 1(b). Hence, some bound states are unoccupied and this gives room for CDW built on the bound states. Let us denote the concentration of unoccupied bound states by δx. It is well established that the hole doping level is pretty close to the concentration of Sr ions; therefore, $\delta x \ll x$. On the other hand, δx is not that small because it is sufficient for VRH. It is reasonable to assume that

$$\frac{\delta x}{x} \sim 0.1. \tag{3}$$

This is the maximum possible relative amplitude for charge density modulation; there are no more quantum states within the impurity band to develop a larger amplitude.

The characteristic VRH temperature T_0 in Eq. (2) depends on doping and sample quality and generally decreases when doping increases (and, thus, conduction becomes easier). At 4% doping, the data of Ref. 4 are well fit with $T_0 \approx 500$ K.[16] Analyzing the curves from, Ref. 5 we have

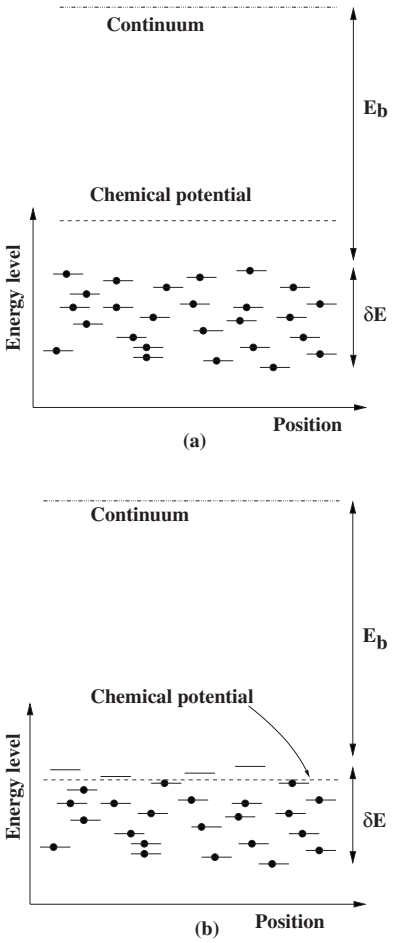

FIG. 1. The diagram of impurity energy levels. (a) The chemical potential is outside the impurity band. (b) The chemical potential is inside the impurity band. $E_b \sim 10-15$ meV is the binding energy and δE is the width of the impurity band.

found $T_0(x=0.02) \sim 8000$ K, $T_0(x=0.03) \sim 2000$ K, and $T_0(x=0.04) \sim 300$ K. The temperature T_0 is related to the 2D density of states G,

$$G = \frac{13.8}{T_0 l^2}, \tag{4}$$

see Ref. 17. Here, l is the localization length (the "Bohr radius" of the bound state). We set the Boltzmann constant equal to unity. The localization length is about 2.5 lattice spacings.[4] Note that the density of states determined in this way is valid up to $T \sim E_b \sim 100-150$ K (ionization of bound states) in spite of the fact that the VRH resistivity formula is valid only up to $T \sim 20-30$ K. The density of states is related to the width of the impurity band δE shown in Fig. 1, $G = x/\delta E$. From here, we find values of δE at different doping levels: $\delta E(x=0.02) \sim 6$ meV, $\delta E(x=0.03) \sim 2$ meV, and $\delta E(x=0.04) \sim 1$ meV.

Spin anisotropies and generation of the second harmonics of the spiral. It is very convenient to use the σ-model notation. The energy density in this notation reads[10]

$$\frac{\rho_s}{2}[\nabla\vec{n}(\mathbf{r})]^2 - \sqrt{2}g\sum_i \vec{\xi}_i\cdot[\vec{n}\times(\boldsymbol{e}_b\cdot\nabla)\vec{n}]\delta(\boldsymbol{r}-\boldsymbol{r}_i)$$

$$+\frac{\rho_s}{2c^2}[D^2 n_a^2(\mathbf{r})+\Gamma_c n_c^2(\mathbf{r})]. \quad (5)$$

Here, $\vec{n}$, $n^2=1$ is the staggered field that describes spins, $\vec{\xi}_i$ is the direction of pseudospin of the ith impurity, $\xi^2=1$, and $\boldsymbol{e}_b$ is the unit vector along the orthorhombic b axis. As we have already mentioned, we neglect here the impurity size. We mention once again that what we call the "impurity" is the occupied bound state. The last two terms in Eq. (5) describe anisotropies induced by the spin-orbit interaction.[18,19] The anisotropies "want" to direct $\vec{n}$ along the b axis. The Dzyaloshinskii-Moriya (DM) vector is $D\approx 2.5$ meV and the XY anisotropy is $\sqrt{\Gamma_c}\approx 5$ meV. The spin-wave velocity is $c\approx\sqrt{2}$ J.

As we described above, the two first terms in Eq. (5) generate the spiral,

$$\vec{n}=[0,\sin(\boldsymbol{Q}\cdot\boldsymbol{r}+\varphi),\cos(\boldsymbol{Q}\cdot\boldsymbol{r}+\varphi)]. \quad (6)$$

Here, we assume that the spins are in the bc plane. However, we will argue below that the actual plane of the spiral is not important; moreover, spins can slowly fluctuate without any static spiral. The disorder and topological defects give random phase φ that broadens the line;[10] however, the broadening is a separate issue and we disregard it here. The XY term in Eq. (5) is $\propto n_c^2=[\cos(\boldsymbol{Q}\cdot\boldsymbol{r}+\varphi)]^2 \to \frac{1}{2}[1+\cos(2\boldsymbol{Q}\cdot\boldsymbol{r}+2\varphi)]\to -\varphi\sin(2\boldsymbol{Q}\cdot\boldsymbol{r})$. Here, we have assumed that $\varphi\ll 1$. Thus, the interaction does not vanish after integration over space only if

$$\varphi = A\sin(2\boldsymbol{Q}\cdot\boldsymbol{r}). \quad (7)$$

This is the mechanism for the generation of the second harmonics in the spin pattern. Substitution of Eq. (6) into Eq. (5) gives the following energy density:

$$\frac{\rho_s}{2}(Q+\varphi')^2 - \sqrt{2}g\sigma(Q+\varphi') - \frac{\rho_s\Gamma_c}{2c^2}\varphi\sin(2\boldsymbol{Q}\cdot\boldsymbol{r}), \quad (8)$$

where $\varphi'=(\boldsymbol{e}_b\cdot\nabla)\varphi$ and $\sigma(\boldsymbol{r})=\Sigma_i\delta(\boldsymbol{r}-\boldsymbol{r}_i)$ is the density of impurities per unit area of the plane. In the case of distribution of states shown in Fig. 1(a), the density of impurities is constant because there is no room for a density modulation, $\sigma=x$. In this case, minimization of Eq. (8) with respect to the amplitude of the second harmonics of the spin spiral gives

$$A=\frac{\Gamma_c}{8c^2Q^2}. \quad (9)$$

The value of A is small, $A\sim 10^{-3}-10^{-2}$, so it is hardly possible to observe it directly in neutron scattering.

Charge density wave. We know that the correct picture of states is shown in Fig. 1(b) and, in this case, the CDW is possible. According to Eq. (5), the energy of a single impurity is shifted due to the second harmonics of φ as

$$\delta\epsilon = -\sqrt{2}g\varphi' = -2\sqrt{2}gQA\cos(2\boldsymbol{Q}\cdot\boldsymbol{r}). \quad (10)$$

Hence, the variation of density of impurities is

$$\delta\sigma = -G\delta\epsilon = B\cos(2\boldsymbol{Q}\cdot\boldsymbol{r}),$$

$$B=2G\sqrt{2}gQA=\frac{13.8}{8l^2x}\frac{\Gamma_c\rho_s}{J^2T_0}\approx\frac{0.3}{l^2x}\frac{\Gamma_c}{JT_0}. \quad (11)$$

Here, G is the density of states given by Eq. (4). By substituting numerical values of parameters in Eq. (11), we find that at $x=0.04$, the amplitude of charge modulation is

$$B\sim 10^{-2}. \quad (12)$$

This value is in units of elementary charge per unit cell of the square lattice. Thus, the modulation is about 20% of the doping level. This dramatic enhancement of the CDW is due to the very high density of states [Eq. (4)]. In doing the estimate, we assumed the static spin spiral in the bc plane [see Eq. (6)]. However, since the effect comes from the phase φ, the static order is not essential. In the case of a fully dynamic spiral, we have to replace in Eq. (11) $\Gamma_c\to\frac{1}{2}(\Gamma_c+D^2)$. Since $\Gamma_c\sim D^2$, this does not influence the estimate [Eq. (12)]. According to Eq. (12), the CDW is so strong that it is quite possible that the real limitation on the amplitude B comes from the available Hilbert space limit given by Eq. (3). Anyway, both estimates [Eqs. (12) and (3)] give a CDW amplitude of about 10% of the doping level.

Interestingly, a naive self-consistent treatment of the mean-field equation [Eq. (8)] gives an instability with respect to the unlimited increase of the CDW amplitude. However, we know from the analysis[9,10] that the stability issue cannot be resolved within the mean-field approximation. This is why here we rely on perturbation theory. In any case, the amplitude is bound from the top by condition (3) and since the perturbation theory result [Eq. (12)] is of the same value as the upper bound, we believe that this is a reliable estimate of the effect. The effect depends on temperature due to the depopulation of the b valley as well as due to the ionization of bound states. The expected dependence is roughly $B\propto\tanh(T_h/2T)$. The characteristic temperature is $T_h\sim 150$ K.

Coulomb interaction, phonons, and large correlation lengths. The mechanism considered above explains the CDW amplitude, but it does not explain large correlation lengths observed in Ref. 3. One needs an additional weak interaction to coordinate the phase of the CDW. There are two candidates for the "coordination interaction": (1) Coulomb interaction and (2) interaction with phonons (lattice deformation). Let us first consider the Coulomb interaction. The dielectric constant κ is strongly anisotropic.[20] For the direction along the c axis, it is equal to the ionic value $\kappa_c\sim 30-70$. The in-plane value is much larger because polarizabilities of impurities contribute to the screening of the electric field.[20] This contribution is proportional to doping, and extrapolating from data,[20] we get that at $x=0.04$, the value is $\kappa_{ab}\sim 2000$. Therefore, for estimates, we will use the effective isotropic dielectric constant that is average between κ_c and κ_{ab}, $\kappa\sim 1000$. Here, we have in mind the zero temperature value.

If the Coulomb interaction is important, then it must establish the CDW antiphase between the CuO_2 layers. On the other hand, we know that the in-plane modulation is very slow, $2\pi/(2Q)\ll d_c$, where $d_c=13.15$ Å is the separation be-

tween the planes. A straightforward electrostatic calculation shows that the Coulomb energy per unit area of the plane in this geometry is $E_C \approx \frac{1}{2\kappa} 3.2 d_c (e\delta\sigma)^2$, where $e\delta\sigma$ is the charge density per unit area, e is the elementary charge, and κ is the dielectric constant (we use CGS units). The density wave is $\delta\sigma = B\cos(2\boldsymbol{Q}\cdot\boldsymbol{r})$. Therefore, with account of the electrostatic energy, the impurity energy shift is changed from Eq. (10) to

$$\delta\epsilon = -2\sqrt{2} gQA \cos(2\boldsymbol{Q}\cdot\boldsymbol{r}) + 3.2\frac{e^2}{\kappa} d_c B \cos(2\boldsymbol{Q}\cdot\boldsymbol{r}). \tag{13}$$

The density variation is $\delta\sigma = -G\delta\epsilon$. Hence, we find from Eq. (13) that the density wave amplitude is

$$B = \frac{2G\sqrt{2} gQA}{1 + 3.2(e^2/\kappa) d_c G}. \tag{14}$$

The difference from Eq. (11) is in the Coulomb factor $F_C = [1 + 3.2(e^2/\kappa) d_c G]^{-1}$. The value of this factor at $x = 0.04$ is $F_C \sim 0.5$. Thus, the Coulomb interaction does not qualitatively influence the estimate [Eq. (12)]. It can change the estimate by at most a factor of ~ 2. This conclusion is supported by the following experimental observation: the CDW amplitude is not very sensitive to temperature up to $T \sim 100-150$ K.[3] On the other hand, the screening must be very sensitive to temperature because at $T=0$, the system is an Anderson insulator, while at $T \geq 50-70$ K, it behaves like a conductor.[5] Thus, the CDW amplitude is not sensitive to the change of the screening regime and, hence, the Coulomb interaction is not important. The most powerful confirmation of this point directly comes from the experiment.[3] In the observed CDW, the layers are in phase and this implies that the Coulomb interaction is negligible.

Thus, as pointed out in Ref. 3, we are left with phonons to coordinate the CDW phase. Most likely, this is also related to the DM interaction. The DM vector D is proportional to the oxygen octahedra tilting angle, so we can write $D \to D + \delta D$, where δD is coupled to the soft phonon responsible for the variation in the tilting angle. The $D^2 n_a^2$ term in Eq. (5) generates coupling to the spiral $D^2 n_a^2 \to (D+\delta D)^2 [\sin(\boldsymbol{Q}\cdot\boldsymbol{r} + \varphi)]^2 \to D\delta D \cos(2\boldsymbol{Q}\cdot\boldsymbol{r} + 2\varphi)$. This generates the lattice deformation at the second harmonics and this is the "coordination" interaction. Clearly, this mechanism gives the same phase of the CDW for nearest CuO_2 layers.

In conclusion, the disordered diagonal spin spiral in the insulating phase of LSCO generates a charge density wave with the wavelength half that of the spin spiral. The charge modulation is due to the relativistic Dzyaloshinskii-Moriya and the XY anisotropies. At $x=0.04$, we estimate the amplitude of the modulation at $\sim 10\%$ of the doping level. The effect survives up to the characteristic temperature $T_h \sim 150$ K. We believe that this theory explains the CDW observed in Ref. 3.

I am grateful to P. Abbamonte and K. Yamada for communicating their results prior to publication. I am also grateful to V. Kotov and A. I. Milstein for helpful discussions.

[1] J. M. Tranquada, B. J. Sternlieb, J. D. Axe, Y. Nakamura, and S. Uchida, Nature (London) **375**, 561 (1995).
[2] N. Ichikawa, S. Uchida, J. M. Tranquada, T. Niemoller, P. M. Gehring, S.-H. Lee, and J. R. Schneider, Phys. Rev. Lett. **85**, 1738 (2000).
[3] A. Rusydi, S. Smadici, J. C. Lee, S. Wang, P. Abbamonte, M. Enoki, M. Fujita, M. Rubhausen, and K. Yamada (unpublished).
[4] B. Keimer, A. Aharony, A. Auerbach, R. J. Birgeneau, A. Cassanho, Y. Endoh, R. W. Erwin, M. A. Kastner, and G. Shirane, Phys. Rev. B **45**, 7430 (1992).
[5] Y. Ando, K. Segawa, S. Komiya, and A. N. Lavrov, Phys. Rev. Lett. **88**, 137005 (2002).
[6] M. Fujita, K. Yamada, H. Hiraka, P. M. Gehring, S. H. Lee, S. Wakimoto, and G. Shirane, Phys. Rev. B **65**, 064505 (2002).
[7] K. Yamada, C. H. Lee, K. Kurahashi, J. Wada, S. Wakimoto, S. Ueki, H. Kimura, Y. Endoh, S. Hosoya, G. Shirane, R. J. Birgeneau, M. Greven, M. A. Kastner, and Y. J. Kim, Phys. Rev. B **57**, 6165 (1998).
[8] O. P. Sushkov and V. N. Kotov, Phys. Rev. Lett. **94**, 097005 (2005).
[9] A. Lüscher, G. Misguich, A. I. Milstein, and O. P. Sushkov, Phys. Rev. B **73**, 085122 (2006).
[10] A. Lüscher, A. I. Milstein, and O. P. Sushkov, Phys. Rev. Lett. **98**, 037001 (2007).
[11] S. A. Kivelson, E. Fradkin, and V. J. Emery, Nature (London) **393**, 550 (1998).
[12] O. P. Sushkov, Wenhui Xie, O. Jepsen, O. K. Andersen, and G. A. Sawatzky, Phys. Rev. B **77**, 035124 (2008).
[13] M. Matsuda, M. Fujita, S. Wakimoto, J. A. Fernandez-Baca, J. M. Tranquada, and K. Yamada, arXiv:0801.2254 (unpublished).
[14] A. V. Chubukov and K. A. Musaelian, Phys. Rev. B **51**, 12605 (1995).
[15] O. P. Sushkov and V. N. Kotov, Phys. Rev. B **70**, 024503 (2004).
[16] E. Lai and R. J. Gooding, Phys. Rev. B **57**, 1498 (1998).
[17] A. L. Efros and B. I. Shklovskii, in *Electron-Electron Interactions in Disordered Systems*, edited by A. L. Efros and M. Pollak (North-Holland, Amsterdam, 1985), p. 409.
[18] J. Chovan and N. Papanicolaou, Eur. Phys. J. B **17**, 581 (2000).
[19] M. B. Silva Neto, L. Benfatto, V. Juricic, and C. Morais Smith, Phys. Rev. B **73**, 045132 (2006).
[20] C. Y. Chen, R. J. Birgeneau, M. A. Kastner, N. W. Preyer, and Tineke Thio, Phys. Rev. B **43**, 392 (1991); C. Y. Chen, E. C. Branlund, C. S. Bae, K. Yang, M. A. Kastner, A. Cassanho, and R. J. Birgeneau, *ibid.* **51**, 3671 (1995).